Nonequilibrium stationary states with ratchet effect

G. Cristadoro[1,2] and D. L. Shepelyansky[2,*]
[1]*Center for Nonlinear and Complex Systems, Dipartimento di Scienze Chimiche, Fisiche e Matematiche, Università dell'Insubria, Via Valleggio 11 and Istituto Nazionale di Fisica della Materia, Unità di Como, 22100 Como, Italy*
[2]*Laboratoire de Physique Théorique, UMR 5152 du CNRS, Université Paul Sabatier, 31062 Toulouse Cedex 4, France*
(Received 20 October 2004; published 11 March 2005)

An ensemble of particles in thermal equilibrium at temperature T, modeled by Nosè-Hoover dynamics, moves on a triangular lattice of oriented semidisk elastic scatterers. Despite the scatterer asymmetry, a directed transport is clearly ruled out by the second law of thermodynamics. Introduction of a polarized zero mean monochromatic field creates a directed stationary flow with nontrivial dependence on temperature and field parameters. We give a theoretical estimate of directed current induced by a microwave field in an antidot superlattice in semiconductor heterostructures.

DOI: 10.1103/PhysRevE.71.036111 PACS number(s): 05.70.Ln, 05.45.Pq, 72.40.+w

According to the second law of thermodynamics there is no stationary directed transport in spatially periodic asymmetric systems in thermal equilibrium [1,2]. However, a time periodic parameter variation may drive such a system out of equilibrium leading to the emergence of stationary transport whose direction depends nontrivially on parameters. Such directed transport appears in systems with noise, fluctuations, and dissipation and is now called Brownian motor or ratchet (see, e.g., reviews [3–5]). The ratchet effect has a generic nature and it has been observed in various physical systems including semiconductor heterostructures [6], cold atoms in a laser field [7], vortices in superconductors [8–10], and macroporous silicon membranes under pressure oscillations [11]. It also has important applications in biological systems as discussed in Refs. [4,12].

In spite of a great recent interest to ratchets the theoretical research is mainly concentrated on one-dimensional models (see, e.g., Ref. [5]). Also, since the ratchet behavior is usually rather complex, an overdamped limit is used very often to obtain analytical parameter dependence even if in this regime a directed transport is absent for ac zero mean force [5]. To understand in a better way the global properties of ratchets and their dependence on such important physical parameters as temperature T and driving strength $\mathbf{f}$, we analyze here a generic case when ac driving affects a Maxwell thermostat ensemble of noninteracting particles moving in an asymmetric two-dimensional (2D) periodic structure. This structure is composed of triangular 2D lattice of rigid semidisks of radius r_d as shown in Fig. 1 (inset). The distance R between disk centers is fixed to be $R=2r_d$ and we assume that collisions with semidisks are elastic. Free particle motion between semidisks is affected by a polarized monochromatic force $\mathbf{f}=f(\cos\theta,\sin\theta)\cos\omega t$ with frequency ω, strength f, and polarization angle θ to the x axis. It is also assumed that particles are in thermal equilibrium and at $f=0$ their velocities are given by the Maxwell distribution at temperature T. Figure 1 shows that in this system ac force generates stationary directed transport. In numerical computations we put r_d, particle mass m, unit of time, and Boltzmann's constant k to be equal to unity.

In order to put particles in thermal equilibrium we choose the elegant method of the Nosè-Hoover thermostat (see, e.g., Refs. [13–15] and references therein). In this method the motion of a particle is affected by an effective friction γ which keeps the average kinetic energy $\langle \mathbf{p}^2/2\rangle$ equal to a given thermostat temperature T. In this way the dynamics of particle is described by the equations

$$\dot{\mathbf{q}}=\mathbf{p}/m, \quad \dot{\mathbf{p}}=\mathbf{F}-\gamma\mathbf{p}, \quad \dot{\gamma}=[\mathbf{p}^2/(2mT)-1]/\tau^2, \qquad (1)$$

where $\mathbf{q}$, $\mathbf{p}$ are particle coordinate and momentum, $\mathbf{F}$ is a sum of ac force and the force of elastic collisions with

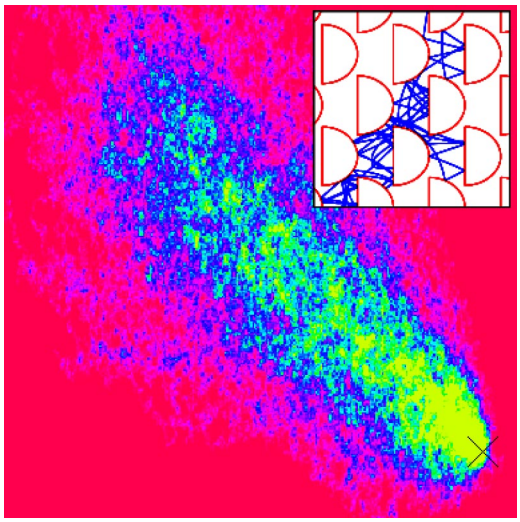

FIG. 1. (Color online) Density distribution averaged over the time interval $0\leqslant t\leqslant 5\times10^5$ and obtained from dynamics of 200 particles given by the Nosè-Hoover equations at thermostat temperature $T=24$. The region of distribution is $x=[-2050,150]$, $y=[-300,1900]$. Initially particles are placed at $x=y=0$ (cross) with random velocities. Density is proportional to color changing from zero (red/black) to maximum (yellow/white). The parameters of driving force are $f=16$, $\omega=1.5$, and $\theta=\pi/8$. The relaxation time scale of the thermostat is $\tau=\sqrt{50}$. The inset shows one trajectory on small scale moving between semidisks.

*http://www.lpt.irsamc.ups-tlse.fr/~dima

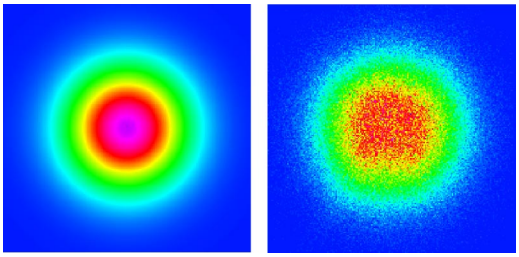

FIG. 2. (Color online) Steady state distribution in 2D momentum plane (p_x, p_y), density is proportional to color changing from zero (blue/black) to maximum (rose-violet/gray). Left: the Maxwell distribution at temperature of Fig. 1; right: distribution obtained numerically from the Nosè-Hoover thermostat for the case of Fig. 1.

semidisks, and τ is the time scale of relaxation to equilibrium.

It is known that the Nosè-Hoover thermostat works well only if the dynamics is sufficiently chaotic [13–15]. In some cases, e.g., for the Galton board, the Nosè-Hoover thermostat gives noticeable deviations from the Maxwell distribution [15]. To check that in our case this method really gives a thermal equilibrium, we analyze the steady state distribution in the momentum space obtained by numerical Runge-Kutta integration of Eqs. (1). Our results show that a small ac force is needed to make chaotic dynamics between semidisks more homogeneous and to produce a stable Maxwell thermal equilibrium which is not sensitive to variation of relaxation rate $1/\tau$ (Fig. 3, inset). At large force the numerical data show that the 2D steady state in the momentum space is still close to the Maxwell distribution (Fig. 2) even if the ac driving produces a clear ratchet effect shown in Fig. 1. The dependence of steady state on temperature closely follows the Maxwell distribution in momentum space $p=|\mathbf{p}|$ as shown in Fig. 3. Thus we may conclude that the dynamics given by the Nosè-Hoover equations allows us to efficiently investigate the effects of ac driving on particles in thermal equilibrium. The numerical data show that this driving generates a strong ratchet effect (Fig. 1) with directed transport wich depends on temperature and parameters of the driving force.

To understand the properties of this directed transport we first analyze the dependence of averaged friction $\langle\gamma\rangle$ on driving strength f and temperature T. The value of $\langle\gamma\rangle$ is obtained by averaging over a long time interval during numerical integration of Eqs. (1) for one trajectory. We also checked that averaging over a few trajectories gives the same result. The data are shown in Fig. 4. They are well described by a global scaling given by

$$\langle\gamma\rangle = Cr_d m^{-1/2} f^2/T^{3/2}. \tag{2}$$

Small deviations seen at low T appear because of a strong driving force which starts to modify significantly the particle velocity distribution in this regime. The numerical constant C is only weakly dependent on θ and ω changing by 50% to 30% when θ changes from 0 to $\pi/2$ and ω changes by a factor 10, respectively. The dependence (2) clearly tells us that in the presence of a driving force the thermostat creates an effective friction force $\mathbf{f}_f = -\langle\gamma\rangle\mathbf{p}$ acting on particle propagation with an effective friction constant $\langle\gamma\rangle$. Surprisingly, this friction coefficient varies with f and T according to Eq. (2) but in a large range remains independent of the relaxation time τ (Fig. 4, inset). We note that the particle dynamics in the absence of a thermostat, but in the presence of friction force $\mathbf{f}_f = -\gamma\mathbf{p}$ with constant friction coefficient γ, has been analyzed in Ref. [16] where it was shown that ac force generates a directed transport on semidisk lattice.

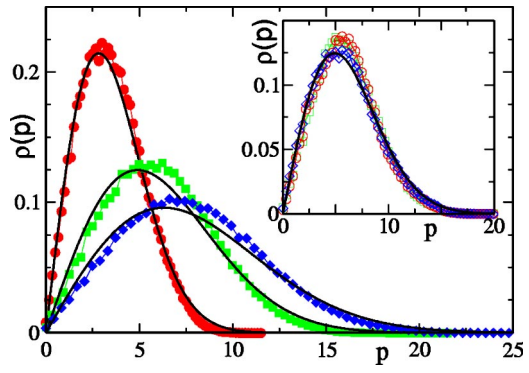

FIG. 3. (Color online) Thermal distribution ρ in momentum $p=|\mathbf{p}|$ for different values of temperature $T=8,16,40$ (from narrow to broad distribution, respectively, shown by curves and symbols). For each temperature value the curve gives the Maxwell distribution and the symbols show the numerical data for the Nosè-Hoover thermostat ($\tau=\sqrt{50}$) in presence of ac driving with parameters of Fig. 1. The inset shows the stability of the Nosè-Hoover thermostat at small ac force ($f=0.5, \omega=1.5, \theta=\pi/8$) with respect to variation of relaxation time $\tau^2=1$ (circles), 50 (squares), 100 (diamonds) at fixed temperature $T=24$; the curve shows the Maxwell distribution. All numerical data are obtained from one long trajectory with $t\leqslant 5\times 10^5$.

To understand the origin of the dependence (2) we put forward the following heuristic arguments. The driving force

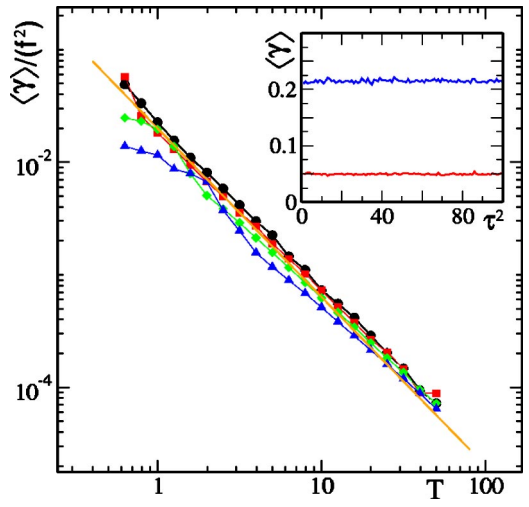

FIG. 4. (Color online) Dependence of rescaled average friction coefficient $\langle\gamma\rangle/f^2$ on temperature T for $f=4$ (circles), 8 (squares), 16 (diamonds), 32 (triangles) (top to bottom) at fixed $\omega=1.5$, $\theta=0$, $\tau^2=50$. The straight line shows dependence (2) with $C=0.02$. The inset shows that $\langle\gamma\rangle$ is robust against variation of τ^2 in the interval [1,100] (with step 1); data are shown for $f=16$, $\omega=1.5$, $\theta=0$, $T=8$ (top curve), and 24 (bottom curve).

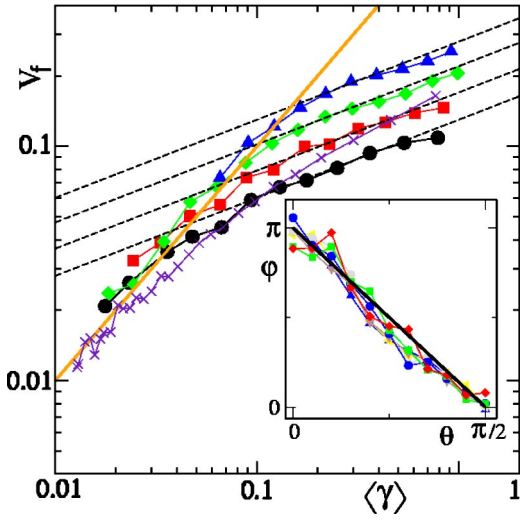

FIG. 5. (Color online) Dependence of the absolute value of average velocity of particle flow v_f on average friction $\langle\gamma\rangle$ for the parameters of Fig. 4 with $f=4$, 8, 16, 32 (same symbols, from bottom to top). Dashed lines show the scaling dependence $v_f \sim (f\langle\gamma\rangle)^{1/3}$ at large $\langle\gamma\rangle$ for different f values; the full line shows scaling $v_f=\langle\gamma\rangle$ at small $\langle\gamma\rangle$. Crosses show data for the same parameters as for squares ($f=8$) but with additional circular scatterer added in the center of unit cell to eliminate orbits with a straight flight through the whole system (see text). The inset shows the dependence of flow direction angle φ on polarization angle θ; data are given for $f=8$, $\omega=1.5$, $\tau^2=50$, and $4\leqslant T\leqslant 11$; full line shows average dependence $\varphi=\pi-2\theta$.

gives a diffusive energy growth during a dissipative time scale $1/\gamma$ so that

$$(\Delta E)^2 \sim D_E/\gamma, \quad D_E \sim f^2 v l, \tag{3}$$

where the diffusion rate in energy is $D_E \sim \dot{E}^2\tau_c \sim f^2 v l$ and the mean-free path $l \sim R \sim r_d \sim 1$ determines the collision time $\tau_c = l/v$. In the Maxwell equilibrium the particle velocity is $v \sim (T/m)^{1/2}$ and the fact that the driving force does not modify the velocity distribution implies that $\Delta E \sim T$ so that the diffusive growth is stopped by effective friction $\gamma \sim D_E/T^2 \sim r_d m^{-1/2} f^2/T^{3/2}$ in agreement with Eq. (2). In fact there is a close relation to results [16] where the thermostat is absent but a friction force $\mathbf{f}_f = -\gamma\mathbf{p}$ with constant γ affects particle dynamics. In that case the ac driving force heats a particle up to energy $E \sim (r_d f^2/m^{1/2}\gamma)^{2/3}$ while in the presence of a thermostat the energy is fixed by temperature $T \sim E$ that imposes a convergence to the stationary state with effective friction given by Eq. (2) [17].

The dependence of average velocity v_f of the ratchet flow on $\langle\gamma\rangle$ for various values of driving strength f is shown in Fig. 5. Globally, the flow velocity v_f grows with increase of γ. Two regimes are clearly seen: $v_f \approx r_d\langle\gamma\rangle$ for $\langle\gamma\rangle < \gamma_c$ and $v_f \approx (r_d^2 f\langle\gamma\rangle/m)^{1/3}/10$ for $\langle\gamma\rangle > \gamma_c \approx f^{1/2}/[30(r_d m)^{1/2}]$. In fact this dependence is very close to the one found in a model with fixed γ [16]. As a result, from Eq. (2) we obtain the dependence of flow velocity on temperature,

$$v_f/v \approx r_d f/50T, \quad (T < T_c); \tag{4}$$

$$v_f/v \approx (r_d f/8T)^2, \quad (T > T_c); \tag{5}$$

where $v=(2T/m)^{1/2}$ is the thermal velocity and $T_c \approx r_d f$ is linked to γ_c obtained from Fig. 5. The transition between two regimes takes place when the energy given by ac force to particle between two collisions becomes larger than thermal energy ($T<T_c$). In that case the effect of driving is strong and $v_f \sim f\tau_c/m \sim r_d f/(mT)^{1/2}$ leading to Eq. (4). For $T>T_c$ thermal fluctuations are strong and the ratchet effect appears only in the second order of force f giving Eq. (5). The numerical factors in Eqs. (4) and (5) are taken for the case $\theta=0$ from Figs. 4 and 5. We note that Eqs. (2)–(5) are derived in the regime of relatively weak friction $\langle\gamma\rangle \ll \omega$ and relaxation rate $1/\tau \ll \omega$. Another important point is that the dependence (4) and (5) is robust with respect to variation of scatter geometry, e.g., the introduction of an additional disk scatterer in the center of the unit cell eliminates all collisionless paths but gives no significant modifications (see Fig. 5).

The dependence of flow directionality, determined through the angle $\varphi[\mathbf{v_f}=v_f(\cos\varphi, \sin\varphi)]$, on the polarization of ac force is shown in Fig. 5 (inset). On average, it is satisfactorily described by the relation $\varphi=\pi-2\theta$ (a similar dependence was seen in Ref. [16]). On a qualitative ground, we may say that at $\theta=0$ due to friction a particle becomes trapped between semidisks of a unit cell that gives a directed transport to the left while for $\theta=\pi/2$ vertical oscillations push particle to the right in the presence of friction. The linear dependence $\varphi=\pi-2\theta$ interpolates between these two limits. However, a more quantitative derivation is needed.

It is interesting to apply the approach developed above to other types of thermostats. It is possible to realize the semidisk Galton board with antidot superlattices for 2D electron gas in semiconductor heterostructures. With such structures the Galton board of disks has already been implemented (see, e.g., Ref. [18]) and effects of microwave radiation has been studied [19]. For disk antidots like those in Refs. [18,19] the ratchet effect is absent due to the symmetry of the antidot. However, for semidisk antidot lattice a strong ratchet effect should appear. To find its properties we should take into account that in this case we have the Fermi-Dirac thermostat with the Fermi energy $E_F \gg T$. Due to that in Eq. (3) the particle velocity v is equal to the Fermi velocity $v_F=(2E_F/m)^{1/2}$ independent of T. This modification gives the average friction γ_F for the Fermi gas,

$$\gamma_F = Cf^2 v_F r_d/T^2 \approx v_f/r_d, \tag{6}$$

where we kept the same numerical constant $C \sim 1/50$. In fact Eq. (6) follows from $D_E \sim f^2 v_F r_d$ [see Eq. (3)] and $\gamma_F \sim D_E/T^2$. The second equality in Eq. (6) appears due to the fact that $E_F \gg T_c$ implying the regime (5) with $v_f \sim \gamma_F r_d$. Of course, only a small fraction T/E_F of electrons near E_F contributes to this ratchet flow. Hence the current I per one semidisk row is

$$I \sim e r_d n_e v_f T/E_F \sim C e r_d^3 \sqrt{n_e} f^2/(T\hbar), \tag{7}$$

where we used that for the 2D electron Fermi gas $E_F=\pi n_e \hbar^2/m$. We note that in semiconductor antidot lattices like in Refs. [18,19] the effective mass m is about 15 times smaller compared to the electron mass. For typical param-

eters of semidisk antidot lattice with electron density $n_e \sim 10^{12}$ cm^{-2}, $r_d \sim 1$ μm, field strength per electron charge $f/e \sim 1$ V/cm and $T \sim 10$ K we obtain $v_f/v_F \sim 10^{-4}$. At these parameters $E_F \sim 150$ K, $v_F \sim 3 \times 10^7$ cm/sec and the current $I \sim 10^{-9}$ A is sufficiently large to be observed experimentally. The result (7) is based on the semiclassical estimate for the diffusion rate D_E which assumes that the energy of microwave photon is larger than the level spacing Δ inside one unit cell: $\hbar\omega > \Delta \approx 2\pi\hbar^2/(mr_d^2)$. In the opposite limit $\hbar\omega \ll \Delta$, ac driving is in the quantum adiabatic regime when the excitation in energy is very weak. Thus for $r_d \sim 1$ μm we have $\Delta \approx 5 \times 10^{-6}$ eV ≈ 0.05 K and the directed transport appears only for $\omega/2\pi > 1$ GHz. In experiments [6] the frequency was deeply in the adiabatic regime with $\omega/2\pi \sim 100$ Hz and the directed transport was absent at zero mean force. We also note that in the quantum case the ratchet transport should disappear as soon as the amplitude of oscillations $f/m\omega^2$ induced by ac force becomes smaller than the wavelength $\hbar/mv_F$ at the Fermi level. Thus the ratchet survives only for $\omega < \sqrt{fv_F/\hbar}$. For field strength of 1 V/cm this gives an approximate bound at 30 GHz.

In summary, we showed that zero mean ac force applied to particles being in thermal equilibrium in asymmetric periodic potential creates a directed transport flow. Its direction is efficiently changed by polarization of the force. We also established the dependence of the flow velocity v_f on temperature and driving field strength for the Maxwell [Eqs. (4)–(6)] and the Fermi-Dirac [Eqs. (6) and (7)] thermostats.

We thank Alexei Chepelianskii, Kvon Ze Don, and Sergey Vitkalov for useful discussions.

[1] M. v. Smoluchowski, Phys. Z. **13**, 1069 (1912).
[2] R. P. Feynman, R. B. Leighton, and M. Sands, *The Feynman Lectures on Physics* (Addison Wesley, Reading, MA, 1963), Vol. 6, Chap. 46.
[3] V. I. Belinicher and B. I. Sturman, Sov. Phys. Usp. **23**, 199 (1980).
[4] R. D. Astumian and P. Hänggi, Phys. Today **55** (11), 33 (2002).
[5] P. Reimann, Phys. Rep. **361**, 57 (2002).
[6] H. Linke, T. E. Humphrey, A. Löfgren, A. O. Sushkov, R. Newbury, R. P. Taylor, and P. Omling, Science **286**, 2314 (1999).
[7] C. Mennerat-Robilliard, D. Lucas, S. Guibal, J. Tabosa, C. Jurczak, J.-Y. Courtois, and G. Grynberg, Phys. Rev. Lett. **82**, 851 (1999).
[8] J. B. Majer, J. Peguiron, M. Grifoni, M. Tusveld, and J. E. Mooij, Phys. Rev. Lett. **90**, 056802 (2003).
[9] J. E. Villegas, S. Savel'ev, F. Nori, E. M. Gonzalez, J. V. Anguita, R. Garcia, and J. L. Vicent, Science **302**, 1188 (2003).
[10] A. V. Ustinov, C. Coqui, A. Kemp, Y. Zolotaryuk, and M. Salerno, Phys. Rev. Lett. **93**, 087001 (2004).
[11] S. Matthias and F. Müller, Nature (London) **424**, 53 (2003).
[12] F. Jülicher, A. Ajdari, and J. Prost, Rev. Mod. Phys. **69**, 1269 (1997).
[13] W. G. Hoover, Phys. Rev. A **31**, 1695 (1985).
[14] W. G. Hoover, *Time Reversibility, Computer Simulation, and Chaos* (World Scientific, Singapore, 1999).
[15] K. Rateitschak, R. Klages, and W. G. Hoover, J. Stat. Phys. **101**, 61 (2000).
[16] A. D. Chepelianskii and D. L. Shepelyansky, cond-mat/0402675.
[17] We note that a numerical constant $C \approx 0.02$ in Eq. (2) (see Fig. 4) corresponds to average dependence $v^2 = 2T = (f^2/\gamma)^{2/3}/7$ from Fig. 5 in Ref. [16].
[18] D. Weiss, M. L. Roukes, A. Menschig, P. Grambow, K. von Klitzing, and G. Weimann, Phys. Rev. Lett. **66**, 2790 (1991).
[19] A. A. Bykov, G. M. Gusev, Z. D. Kvon, V. M. Kudryashev, and V. G. Plyukhin, Pis'ma Zh. Eksp. Teor. Fiz. **53**, 407 (1991) [JETP Lett. **53**, 427 (1991)].